ACS APPLIED MATERIALS & INTERFACES

Research Article

www.acsami.org

Modification of the Active Layer/PEDOT:PSS Interface by Solvent Additives Resulting in Improvement of the Performance of Organic Solar Cells

Olesia Synooka,*[,†] Florian Kretschmer,[‡,§] Martin D. Hager,[‡,§] Marcel Himmerlich,[†] Stefan Krischok,[†] Dominik Gehrig,[⊥] Frédéric Laquai,[⊥] Ulrich S. Schubert,[‡,§] Gerhard Gobsch,[†] and Harald Hoppe*[,†]

[†]Institut für Physik and Institut für Mikro- und Nanotechnologien, Technische Universität Ilmenau, Langewiesener Strasse 22, 98693 Ilmenau, Germany

[‡]Laboratory of Organic and Macromolecular Chemistry (IOMC), Friedrich-Schiller-University Jena, Humboldtstrasse 10, 07743 Jena, Germany

[§]Jena Center for Soft Matter (JCSM), Friedrich-Schiller-University Jena, Philosphenweg 7, 07743 Jena, Germany

[⊥]Max Planck Research Group for Organic Optoelectronics, Max-Planck-Institute for Polymer Research, Ackermannweg 10, D-55128 Mainz, Germany

ABSTRACT: The influence of various polar solvent additives with different dipole moments has been investigated since the performance of a photovoltaic device comprising a donor−acceptor copolymer (benzothiadiazole-fluorene-diketopyrrolopyrrole (BTD-F-DKPP)) and phenyl-C_{60}-butyric acid methyl ester (PCBM) was notably increased. A common approach for controlling bulk heterojunction morphology and thereby improving the solar cell performance involves the use of solvent additives exhibiting boiling points higher than that of the surrounding solvent in order to allow the fullerene to aggregate during the host solvent evaporation and film solidification. In contrast to that, we report the application of polar solvent additives with widely varied dipole moments, where intentionally no dependence on their boiling points was applied. We found that an appropriate amount of the additive can improve all solar cell parameters. This beneficial effect could be largely attributed to a modification of the poly(3,4-ethylenedioxythiophene):poly(styrenesulfonate) (PEDOT:PSS)-active layer interface within the device layer stack, which was successfully reproduced for polymer solar cells based on the commonly used PCDTBT (poly[*N*-900-hepta-decanyl-2,7-carbazole-*alt*-5,5-(40,70-di-2-thienyl-20,10,30-benzothiadiazole)]) copolymer.

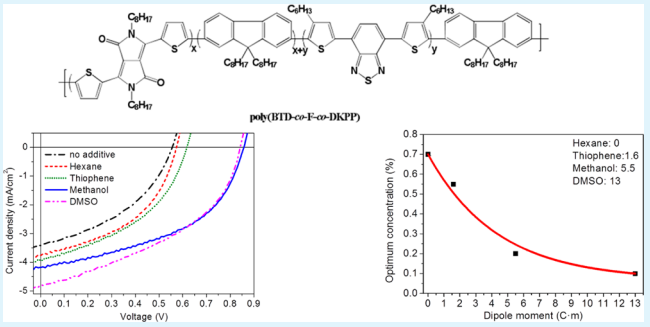

KEYWORDS: *additives, dipole moment, copolymer, solar cell, PEDOT:PSS, morphology*

1. INTRODUCTION

For many years sun light was only used as an indirect energy source. In contrast, today organic photovoltaic cells (OPVs), which can convert sunlight directly to electrical power, have attracted growing attention due to their unique advantages, such as potential for low cost, easy fabrication, low weight, and high flexibility.[1−6] However, for industrialization of organic solar cells (OSCs) their performance and lifetime have to be further optimized.[7]

Currently, the most successful approach yielding high polymer solar cell performances is based on donor−acceptor bulk-heterojunctions (BHJ). In BHJ the photoactive layer consists of an intimate mixture of a conjugated polymer-based electron donor and a fullerene-based electron acceptor deposited from a mixed solution using common solvents.[8,9] As the solvent evaporates and the film dries, the donor (D) and acceptor (A) components phase-separate into different domains.[10] The resulting efficiency of the solar cell is extremely dependent on the size, composition, and crystallinity of these domains and thus critically depends on the nanomorphology of the photoactive layer.[11−13] More recently, several approaches for controlling the bulk heterojunction morphology have been reported, including adjusting the rate of film-formation process[14] using a cosolvent,[15] solvent vapor annealing,[16,17] microwave annealing,[18] and thermal annealing.[19,20] Although, local ordering, crystalline phases and bicontinuous structures could be obtained,[21−24] it is challenging to transfer these methods to industrial fabrication processes.

Another approach for controlling the bulk heterojunction nanomorphology is the incorporation of a small amount of high boiling point (T_b) solvents into the D/A solution.[25−30] Bazan et al. reported a significant performance improvement to efficiencies above 5% in blends of $PC_{71}BM$ with a low band gap polymer poly[2,6-(4,4-*bis*(2-ethylhexyl)-4*H*-cyclopenta[2,1-*b*;3,4-*b*′]dithiophene)-*alt*-4,7-(2,1,3-benzothiadiazole)] (PCPDTBT) upon the addition of a few volume percent of either alkanedithiols or alkanedihalides.[31−33] Similar improvements were recently reported for other low-bandgap polymers, where the morphologies cannot be optimized by conventional thermal annealing processes.[34−36] Morphological studies and photophysical measurements performed on these systems have revealed that the

Received: December 18, 2013
Accepted: June 19, 2014
Published: June 30, 2014

Scheme 1. Schematic Representation of the Polymer Synthesis Routine of BTD-F-DKPP (x = 0.3, y = 0.7) with HOMO and LUMO Values of the Initial Monomers and the Resulting Polymer Determined by CV

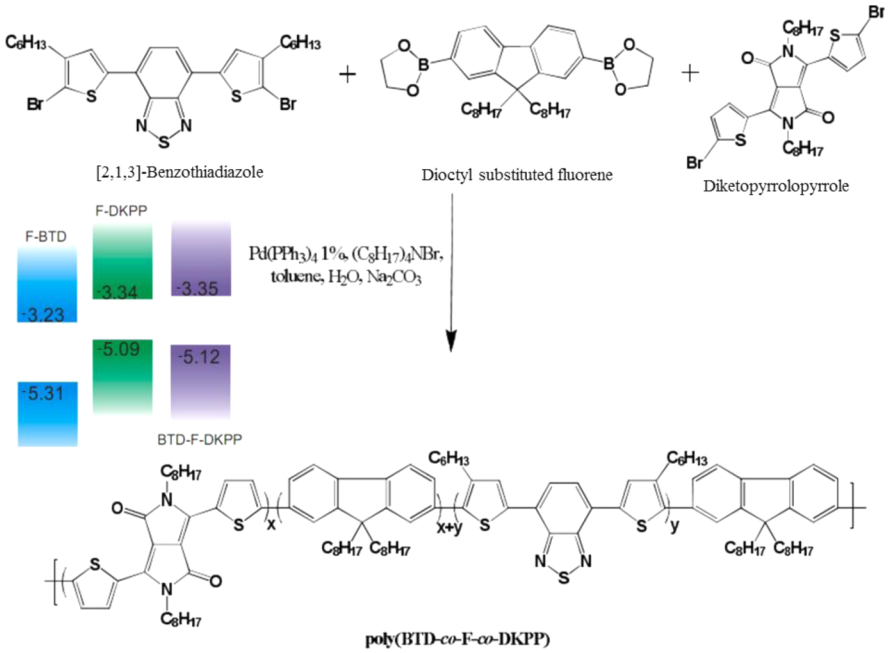

improvement in the device performance had to be related mainly to improved phase separation within the blend film, giving rise to an enhancement in the photoconductivity of the free charge carriers.[37]

Moreover, Seo et al.[38] have demonstrated that the solar cell device performance can be markedly improved via incorporation of a conjugated polyelectrolyte (CPE) interlayer deposited on top of the photoactive layer from a methanol solution. This improvement was attributed to local dipole arrangements, modifying the contact with the electron extracting aluminum electrode. Furthermore, the authors showed that deposition of methanol alone on top of the active layer similarly increased the open circuit voltage and device performance to a somewhat lower extend. Therefore, the performance improvement was attributed to a combination of two effects: methanol treatment and the presence of the thin CPE layer. A more recent in-depth investigation by Zhou et al.,[39] methanol top-casting on PTB7:$PC_{70}BM$ revealed a passivation of surface traps, leading to reduced recombination as well as increased built-in voltage and surface charge density of the methanol treated devices, which could not be related to any change in the blend composition or morphology. The origin of the surface trap reduction, however, remained open and is subject of further investigations. Furthermore, it was shown by Liu et al.[40] that the simple ethanol spin-casting on top of the active layer also results in improvements of solar cell performance. The authors demonstrated that ethanol can penetrate through the PCX3/$PC_{71}BM$ and considerably influence the contact properties of a "buried" interface. These positive changes were noticed only in case of using PEDOT:PSS and were not confirmed in case of using MoO_x. However, no further investigations of the active layer-PEDOT:PSS interface were presented. Furthermore, Wang et al.[41] demonstrated improved electron injection upon polar solvents (methanol or ethanol) spin-casting of on top of an organic layer of a light emitting diode (OLED). They found that the removal of the solvent did not occur easily even in vacuum. Therefore, the authors concluded that solvent treatment of the organic active layer can effectively modify the organic/metal cathode interface.

Intrigued by the performance improvement upon the bare methanol treatment, we applied methanol to our material system as well, composed of a novel donor−acceptor statistical copolymer based on polyfluorene (PFO) as donor and benzothiadiazole (BTD) or promissing diketopyrrolopyrrole (DKPP)[42,43] as acceptor units. To adjust the optical and electrical properties for optimal performance, the ratio between the accepting units has been varied systematically earlier.[44] However, since deposition of methanol on top of the photoactive layer is complicated within continuous solar cell production, we used methanol as solvent additive, as well. Methanol applied as a solvent additive might potentially modify both: the bulk heterojunction morphology and interfaces to charge collecting electrodes. Furthermore, as the performance change in those photovoltaic devices cannot be assigned to the effect of higher boiling point solvent additions, we considered a variation of solvent additives exhibiting largely varying dipole moments. Hence, hexane, thiophene, methanol, and dimethyl sulfoxide (DMSO) were chosen to vary the polarity of solvent additives by dipole moments between 0, 1.6, 5.5, and 13 C·m, respectively.[45] Among these solvent additives, only DMSO has a boiling point higher than the host solvent chlorobenzene. For distinguishing the effects, we conducted optical, electrical, morphological and surface characterizations on solar cells and individual layers. Our investigation revealed that a large part of the performance improvement has to be assigned to a change in the active layer-PEDOT:PSS interface. Furthermore, corresponding improvements upon polar solvent addition have been confirmed with more efficient PCDTBT-based solar cells as well.

2. EXPERIMENTAL SECTION

2.1. Materials. Scheme 1 shows the synthesis of the BTD-F-DKPP statistical D-A-copolymer, consisting of fluorene as donor-group and either BTD or DKPP as acceptor groups. The three monomers BTD, F, DKPP were synthesized as described in ref 44. The yields for the alkylation of the DKPP were generally in the lower range (~30%) compared to that reported in the literature (11−76%). The unbrominated BTD monomer was prepared via a Suzuki cross coupling reaction in the microwave with 84% yield. A Suzuki cross coupling was utilized for the polymerization, 1 equiv fluorene (F) was used as connecting unit and the other comonomers were used in a ratio of 3:7 (BTD:DKPP) and purified by precipitation, Soxhlet extraction, and repeated precipitation. The yield of the polymer achieved was 77%. SEC measurements revealed a molar mass (M_n) of 25 000 g/mol with a PDI value of 2.18. The HOMO level was located at −5.12 eV, and the LUMO level, at −3.35

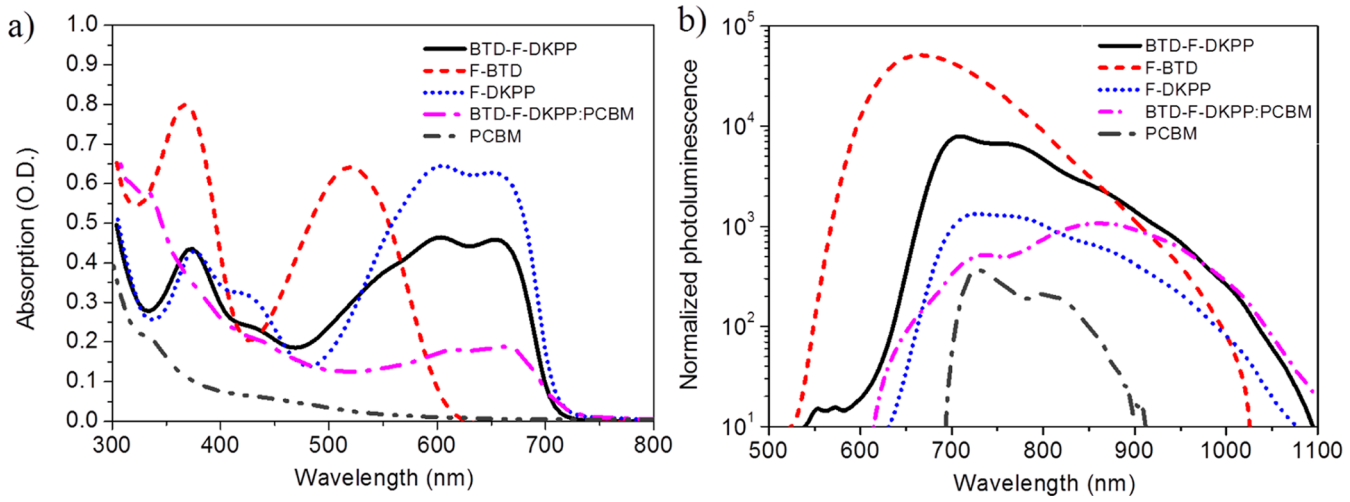

Figure 1. (a) Optical absorption and (b) photoluminescence normalized to the absorption at laser excitation wavelength (445 nm) of pristine terpolymer BTD-F-DKPP, its monomers (F-BTD, F-DKPP), and PCBM as well as BTD-F-DKPP:PCBM blend films.

eV below the vacuum level resulting in band gap of 1.77 eV defined by cyclic voltammetry (CV).

Poly(3,4-ethylenedioxythiophene):poly(styrenesulfonate) (PEDOT:PSS) (CLEVIOS, Hereaus) was employed as a hole transporting layer.

2.2. Device Fabrication and Characterization. Solar cell device preparation involved etching part of the ITO-layer on glass for selectively contacting the back electrode, followed by cleaning in ultrasonic bath using acetone and isopropanol. PEDOT:PSS was spin-cast from aqueous solution on top of ITO and served as the hole transporting layer. It was annealed on the hot plate for 15 min at 180 °C in order to drive the water out of the film. The photoactive layer was prepared from BTD-F-DKPP:PCBM chlorobenzene solutions with 1:4 polymer:fullerene blending ratios. For the additive containing solutions, hexane, thiophene, methanol and DMSO were added in different concentrations into the BTD-F-DKPP:PCBM chlorobenzene solution. Solutions were stirred overnight at 45 °C in a N_2 glovebox and then spin-cast on top of the PEDOT:PSS layer. For the top electrodes, 50 nm of magnesium and 100 nm of aluminum were deposited sequentially by thermal evaporation, resulting in solar cells with an active area of 0.5 cm^2. All samples were encapsulated under glass prior to characterization.

Current−voltage (J−V) measurements of the solar cell devices were performed under a class A AM1.5 solar simulator and were recorded with a Keithley 2400 source-measure-unit. External quantum efficiencies (EQE) were recorded under monochromatic light with an additional halogen bias light, providing an excitation intensity of about one sun. Electroluminescence (EL) spectra were recorded using fiber spectrometers and electrical excitation by a 50 mA injection current.

For charge carrier mobility determination, a single carrier space charge limited current (SCLC) devices in diode configuration were prepared, using a layer stack of glass/ITO/PEDOT:PSS/active layer/Au. ITO coated glass substrates were etched at the region of contact to the Au and subsequently cleaned in acetone and isopropanol. Thereafter, a layer of PEDOT:PSS (~30 nm) was spin coated onto the substrates. After drying the PEDOT:PSS for 15 min at a temperature of 180 °C, 250 nm thick layers of unmodified or additives-modified BTD-F-DKPP:PCBM were spin-cast on top under inert conditions. The top Au electrodes were thermally evaporated onto the active layer under high vacuum conditions defining an active area of 0.16 cm^2 for a single SCLC device. The devices were encapsulated using glass and an epoxy resin under inert environment. The devices were characterized in the dark at room temperature with a Keithley 2400 source measure unit. Because of the symmetrical work function electrodes in hole-only devices, built-in voltage (V_{bi}) close to 0 V was assumed for fitting measured J−V characteristics. The series resistance was determined from the reference devices fabricated without the active layer and was found to be 5.3 Ω. Both the V_{bi} and the voltage drop (IR) over the series resistance were subtracted prior to fitting the measured J−V characteristics using the Murgatroyd SCLC relationship for mobility determination.[46]

2.3. Film Characterization. Absorption spectra were obtained from transmission and reflection spectra recorded on a Varian Cary 5000.

Steady-state photoluminescence spectra were recorded using fiber spectrometers and optical excitation by laser light at 445 nm. For time-resolved photoluminescence studies, transient emission spectra on a picosecond time scale were recorded with a Streak Camera System (Hamamatsu C4742) in fast sweep mode. The excitation wavelength of 400 nm was provided by a frequency-doubled output of a Ti:sapphire femtosecond oscillator system. Detection of nanosecond time scale emission spectra was performed with the same Streak Camera System but in slow sweep mode, while the excitation of 400 nm was provided by frequency doubling the output of a commercial femtosecond amplifier laser system (Coherent LIBRA-HE).

Topography scans and thickness measurements were performed using a Dimension 3100 Nanoscope atomic force microscope (AFM) in tapping mode.

Scanning electron microscopy (SEM) measurements of the cross-section of ITO/PEDOT:PSS/active layer films were made using Hitachi S 4800.

The surface properties of the unmodified and additive-modified PEDOT:PSS films were characterized, after transfer of the samples in inert gas from the glovebox to the UHV system, by X-ray and ultraviolet photoelectron spectroscopy (XPS, UPS) in normal emission employing monochromated Al Kα

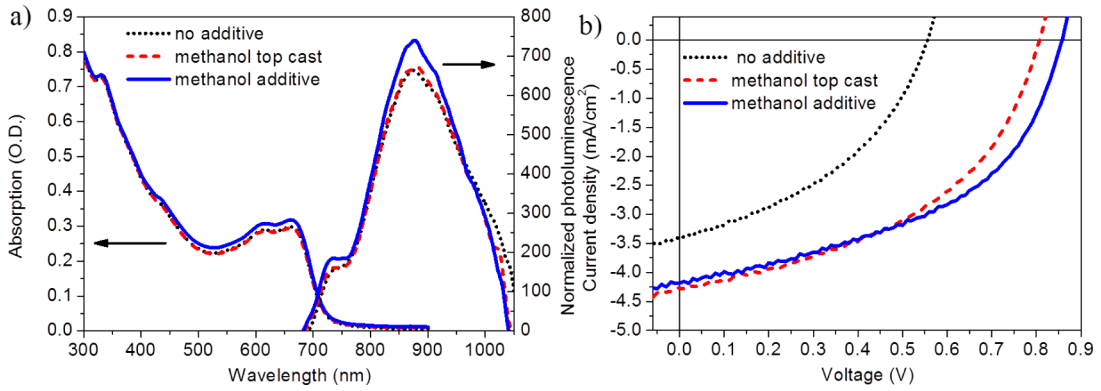

Figure 2. (a) UV−vis absorption spectra and normalized photoluminescence of BTD-F-DKPP films and (b) *J*−*V* characteristics of the same films in solar cell devices, spin-cast from solution as pristine film, or either with methanol on top of the active layer or with methanol applied as additive in solution.

radiation ($h\nu$ = 1486.7 eV) as well as ultraviolet radiation (He I − $h\nu$ = 21.2 eV and He II − $h\nu$ = 40.8 eV) for electron excitation.[47,48] The measured values of the work function and the ionization potential were evaluated as the difference between vacuum level and Fermi level as well as between the onset of an occupied states and Fermi level, respectively. XPS provides information about up to the first 10 nm of the layer under investigation and hence is capable of probing the surface material composition.

3. RESULTS AND DISCUSSION

At first we investigated the optical properties of F-BTD, F-DKPP, and BTD-F-DKPP copolymers, PCBM, and blends of BTD-F-DKPP:PCBM in thin films. As summarized in Figure 1a, the two base copolymers, F-BTD and F-DKPP, exhibited considerably different optical band gaps of 2.08 and 1.75 eV, respectively. The statistical terpolymer BTD-F-DKPP, consisting 30% BTD and 70% DKPP acceptor units, yielded an additive and strong absorption in the range between 500 and 700 nm. Also blending of BTD-F-DKPP with PCBM resulted in additive absorption in thin films. Photoluminescence spectra (Figure 1b) normalized to the absorption at the laser excitation wavelength (445 nm) demonstrate that F-BTD exhibited an approximately 50 times larger photoluminescence signal as compared to F-DKPP. The photoluminescence spectrum of the BTD-F-DKPP copolymer shows the expected additive behavior, resulting in intermediate photoluminescence strength. Upon addition of PCBM and formation of a bulk heterojunction the photoluminescence is reduced by a factor larger than 10, indicating >90% exciton dissociation efficiency. However, a very strong signal, centered at 875 nm, occurred in addition to the quenched polymer and fullerene photoluminescence, which indicates strong charge-transfer (CT) state recombination across the heterojunction. This may be either due to geminate or bimolecular radiative recombination and puts a strong limitation on the accessible photocurrent generation.[49,50]

The UV−vis absorption and photoluminescence spectra of BTD-F-DKPP:PCBM films, either spin-cast from blend solutions without or with methanol additive and, alternatively, with methanol spin-cast on top of the active layer are presented in Figure 2. The optical properties of the films with methanol spin-cast on top of the active layer and from solution with a small amount of methanol, varied negligibly as compared to the active layer cast from the unmodified solution. Since, generally, the photoluminescence signals can be scaled with the domain size, as for larger domain sizes the probability of reaching the heterojunction interface and thus the probability for exciton splitting decreases due to the limited lifetime of excitons,[15] no variation in signal strength of the photoluminescence signals at 700−750 and 750−1000 nm might indicate no modifications of the bulk heterojunction morphology (degree of phase separation). In addition, no significant change in the CT-state recombination was observed at the peak wavelength of 875 nm. This might further confirm that the blend morphology remained almost unaffected by the methanol treatments.

However, even though no clear indications of a possible morphological change or a change in the CT-recombination could be detected, the photovoltaic performance was increased remarkably comparing the untreated pristine active layer and the active layer with methanol spin-cast on top as well as the devices with methanol additive (compare Figure 2b). Both methanol applications, on top of the photoactive layer and addition into solution, resulted in a significant increase of the photocurrent and open circuit voltage. Using methanol as an additive yielded a slight further improvement of the open circuit voltage. The increased photocurrent might be an indication of more efficient charge carriers extraction and, as noticed before by Zhou et al.,[39] reduction of interface recombination upon applying methanol in both ways. However, as both of the methanol treatments did not reduce the CT-PL peak, the effect of the current increase may thus be exclusively assigned to the interfacial modifications. Since the photocurrent density only yielded about 5 mA/cm^2 in the best case, it appears that a large amount of the charge carriers are tightly bound across the heterojunction, comparing the experimental photocurrents with expected from optical absorption. From photocurrent data (not shown) it can be concluded that about 50% of the current losses found at the short circuit condition have to be related to bimolecular recombination losses.

A remarkable increase in the open circuit voltage has been earlier assigned to a modification of the photoactive layer blend composition near the charge extracting electrodes.[51] This might further indicate that in our case the modification was taking place mostly near the electrodes. Furthermore, the considerable increase in open circuit voltage earlier observed by Zhou et al.[39] and Liu et al.[40] after simple spin-casting polar solvents on top of the active layer was also attributed to the modification of the BHJ/metal cathode interface with a decrease of the injection barrier and passivation of the surface traps.

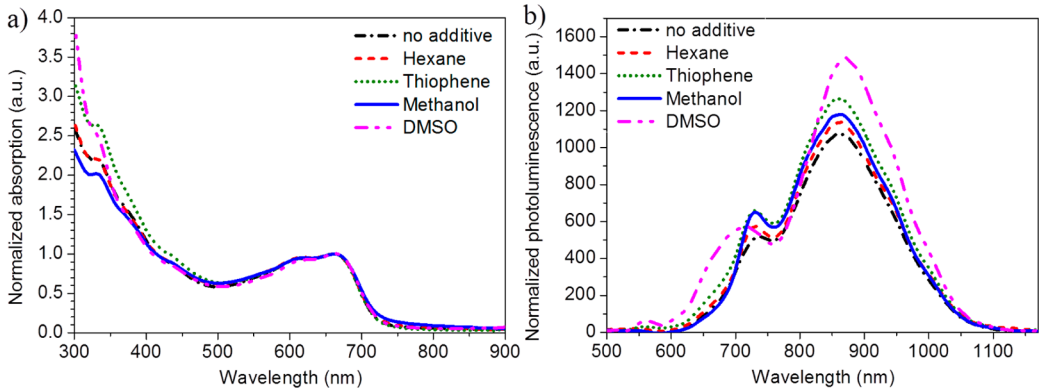

Figure 3. (a) UV−vis absorption and (b) normalized photoluminescence spectra of BTD-F-DKPP:PCBM blend films without and with various processing additives with varying dipole moments.

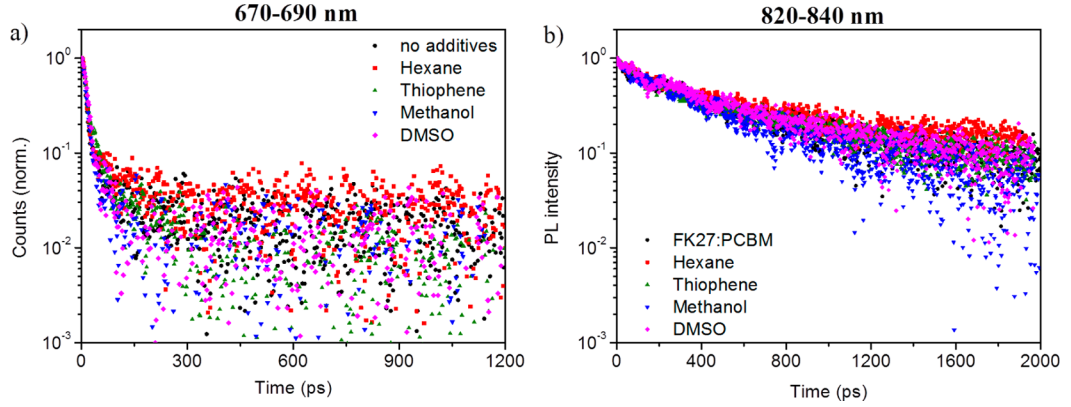

Figure 4. Fluorescence transients of blend films spin-coated from solutions without and with additives. The emission was integrated between (a) 670−690 nm (polymer singlet emission) and (b) 820−840 nm (CT-state emission). Samples were excited at 400 nm with a femtosecond laser pulse.

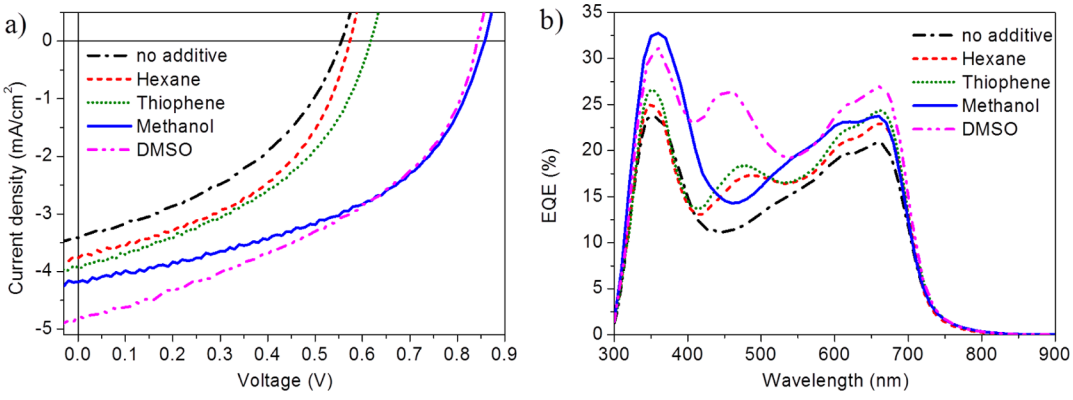

Figure 5. (a) *J*−*V* characteristics of solar cells modified with different additives and (b) the corresponding external quantum efficiencies.

In contrast to other additives, methanol is unlikely to selectively dissolves one of the active layer components as the solubility of conjugated polymers and fullerene derivatives is generally low in methanol. However, it is a polar solvent, which might result in a polarization effect within the modified solution or in bulk heterojunctions. To check this hypothesis and in order to gain larger contrast between the additive and the host solvent chlorobenzene, which has a rather comparable polarity (5.2 C·m) to methanol, we chose several additional solvent additives with largely varied dipole moments between 0 (hexane), 1.6 (thiophene), 5.5 (methanol), and 13 C·m (DMSO)[45] and investigated their influence on solar cell performance and optical properties. It should be noticed that while BTD-F-DKPP is completely insoluble in methanol and DMSO and has low solubility in hexane (<1 mg/mL), its solubility is somewhat higher in thiophene (∼10 mg/mL). Inspecting the optical absorption of the additive modified BTD-F-DKPP:PCBM bulk heterojunctions did not reveal significant changes as compared to the unmodified active layer except for some variation in PCBM absorption at ∼350 nm (Figure 3a). However, in case of DMSO most prominently the PL (Figure 3b) was increased between 600 and 700 nm as well as between 800 and 1000 nm in comparison to all other films. Thus, the possible considerable modification of the bulk heterojunction morphology might be expected only in the case of DMSO,

Table 1. Photovoltaic Performance and Hole Mobility of the BHJ Solar Cells Composed of BTD-F-DKPP:PCBM Fabricated with Various Processing Additives (EQE Corrected Data)

BTD-F-DKPP:PCBM + additive	dipole moment (C·m)	boiling point (°C)	% in host solution	J_{SC} (mA/cm^2)	V_{OC} (mV)	FF (%)	PCE (%)	PCE max (%)	R_S (Ω)	R_P (Ω)	μ_h (cm^2/ Vs)
chlorobenzene (host)	5.2	131		3.4 ± 0.1	541 ± 5	41.8 ± 1.0	0.77 ± 0.01	0.78	9	925	1.3×10^{-6}
hexane	0.0	68	0.8	4.1 ± 0.1	558 ± 7	46.4 ± 2.0	0.92 ± 0.06	0.98	6.8	908	1.6×10^{-6}
thiophene	1.6	84	0.55	4.1 ± 0.3	575 ± 7	46.6 ± 2.0	1.0 ± 0.03	1.13	8.2	947	1.4×10^{-6}
methanol	5.5	65	0.2	4.7 ± 0.2	843 ± 5	50.7 ± 3.0	1.67 ± 0.04	1.73	8.9	1301	1.8×10^{-5}
DMSO	13.0	189	0.09	4.8 ± 0.3	837 ± 10	42.9 ± 3.0	1.62 ± 0.08	1.70	8.5	950	2.1×10^{-5}

whereas all other solvent additives result in almost identical optical properties.

Furthermore, time-resolved photoluminescence measurements (Figure 4) confirmed and supported the results and conclusions obtained by steady state PL. The PL decay dynamics do not vary significantly and indicates only minor changes of domain sizes and thus—if at all—only minor changes of the blend morphology. The emission at 670−690 nm from blend films spin-cast from solution with and without additives allowed measuring the quenching of polymer singlet exciton (Figure 4a). The excitation lifetimes were estimated based on the monoexponential fits of the integrated intensity in this wavelength region as 12.9 ps for the untreated film, 14.1 ps for the film modified by hexane and 17.9 ps for thiophene, 13.8 ps for methanol as well as 16.3 ps for DMSO. Interestingly, the emission between 820 and 840 nm (shown in Figure 4b) is below the optical bandgap and thus appears to originate from a long-lived species, which emission is extending into the NIR. Hence, this emission was assigned to CT state photoluminescence.

Figure 5a shows the $J-V$ characteristics of BTD-F-DKPP:PCBM BHJ solar cells processed using the various additives. We found that photovoltaic cells based on BTD-F-DKPP:PCBM processed with polar additives generally exhibited improved photovoltaic parameters for increasing polarity as compared to the unmodified blend. The data obtained from Figure 5 are summarized in Table 1, including EQE-corrected photocurrents and device-to-device variation, collected from ∼200 devices per parameter. The thickness of the active layer without any additives was optimized to yield the best solar cell performance and determined as ∼55 nm. Upon using the additives the resulting active layer thickness was varying within about ±10% (hexane, thiophene ∼50 nm; DMSO ∼47 nm; methanol ∼60 nm)—justifying the comparability between these different films.

The $J-V$ curves clearly show a notable improvement of the photovoltaic performance upon additives incorporation. The best cells with methanol as an additive exhibited 1.73% power conversion efficiency, while cells without any additives revealed only 0.78%. The strongest improvement for the additive modified devices was found in a 55% increase of the open circuit voltage from about 550 to 850 mV in case of methanol and DMSO. In Figure 5b the additional peak occurring between 400 and 500 nm for hexane, thiophene, and DMSO in the EQE spectrum can most probably be assigned to a light interference effect as no significant change of absorption upon additives treatment was observed. The highest photocurrent increase of about 40% was obtained for DMSO and reached 4.8 mA/cm^2, as derived from the EQE-spectrum. As the short circuit current is generally associated with the charge carrier mobility, the SCLC method was used in order to investigate possible changes in the hole mobility upon treatment with additives. It should be noticed that devices composed of BTD-F-DKPP copolymer have generally low hole mobility (Table 1). The addition of small amounts of hexane and thiophene has almost no effect on the hole mobility. In contrast, methanol and DMSO additives resulted in an increase in the hole mobility by 1 order of magnitude.

Interestingly, the optimum concentration of the additives, which was used to achieve the best photovoltaic parameters, was found to decay exponentially with the additive's dipole moment (Figure 6). However, ethanol, which was also

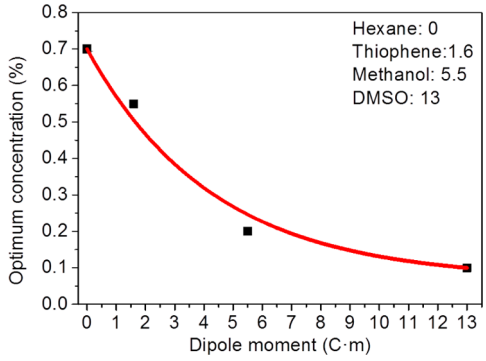

Figure 6. Dependence of the optimum additive concentration on its dipole moment (a decaying exponential function was used for fitting).

investigated during this study, did not follow this trend, even though it has a comparable dipole moment (5.7 C·m) with methanol. The reasons for that have to be further investigated and are beyond the scope of the present study.

In order to gain more insight into charge injection and recombination, electroluminescence (EL) measurements were performed on these solar cells. During the measurements, the detected luminescence signal was controlled by the injection current without any pumping light. This allows avoiding completely potential excitation light contributions. Generally, as electrons and holes are injected into the device, they must recombine either radiatively or nonradiatively. The first state that allows for recombination must be the lowest energetic state, which for BHJs is the charge transfer (CT) state. Consequently, EL allows directly access the CT-state within the terpolymer:PCBM blends. Even though, there remains the probability to excite the individual materials luminescence, both, the higher injection probability of electrons into the LUMO of the PCBM and an energetically favorable charge transfer from the LUMO of the terpolymer into the PCBM basically result in a population of the PCBM-LUMO state and thus only the CT-state recombination is observed in case of the

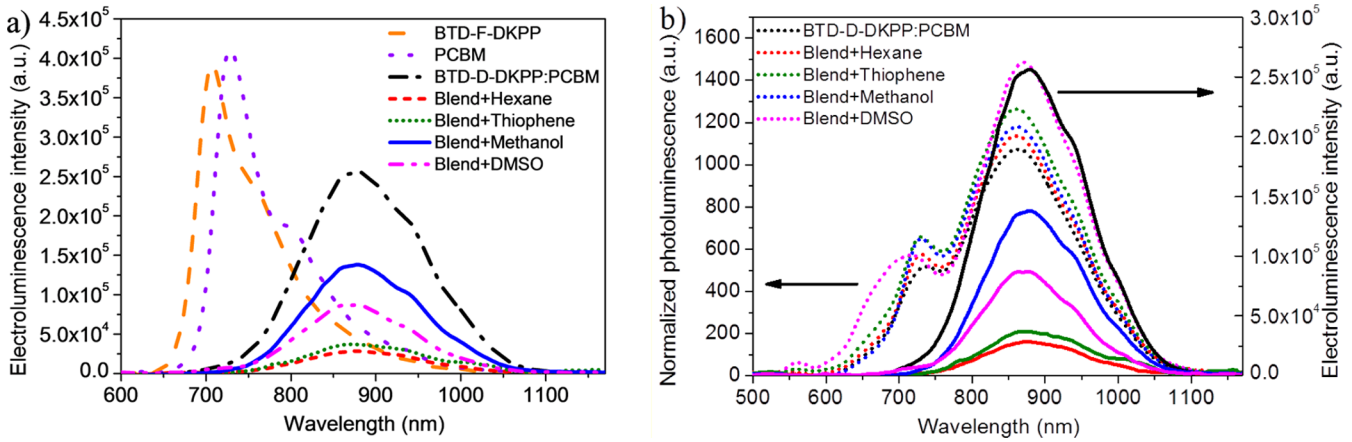

Figure 7. (a) EL spectra of the pristine components and of the blends, which show a dominant CT-state recombination without (black) and with different additives (measured with constant current 50 mA). (b) Comparison of the EL and PL spectra to confirm observation of the CT.

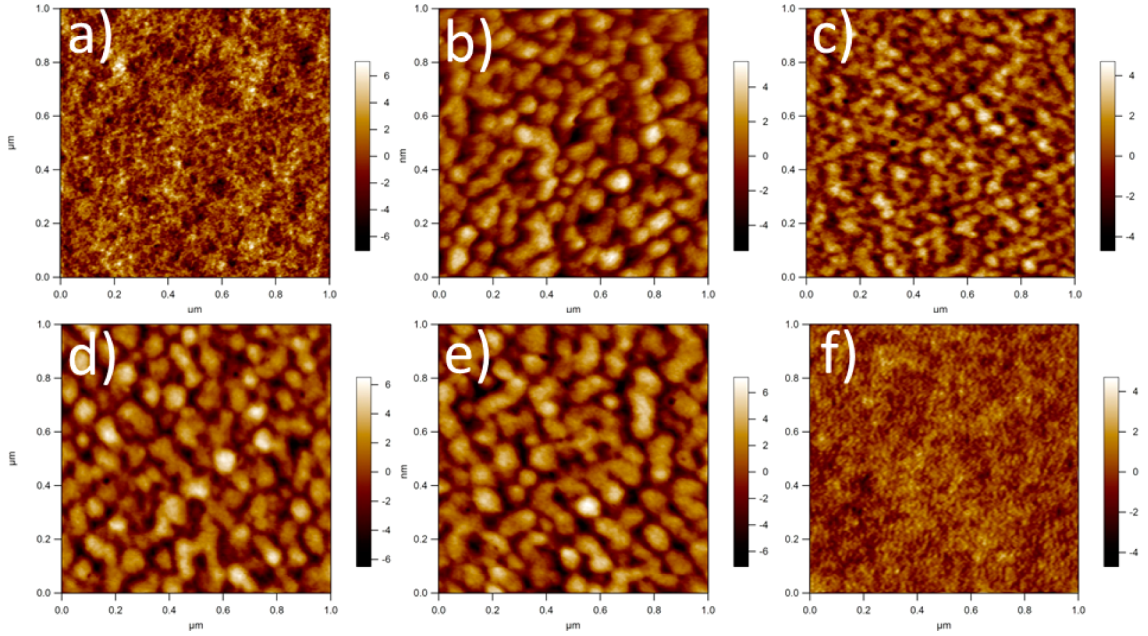

Figure 8. AFM images of films cast from pristine BTD-F-DKPP (a) and blend films cast from BTD-F-DKPP:PCBM without (b) and with hexane (c), thiophene (d), methanol (e), and DMSO (f) additives.

blends.[50] Figure 7 shows the electroluminescence (EL) spectra of BTD-F-DKPP:PCBM solar cells and pristine BTD-F-DKPP as well as pristine PCBM. In case of the blend neither the polymer nor the PCBM EL excitation was observed. Interestingly, the BTD-F-DKPP:PCBM devices with additives displayed significantly lower CT state EL intensities compared to the unmodified blend. This strong lowering of the radiative CT-state recombination is not in accordance with the reciprocity relation postulated for solar cells in general, as improved solar cell performance should be accompanied by improved ratio of the radiative to the nonradiative recombination.[52,53] Hence, the additives do not only increase the photocurrent but also lower the electroluminescence through the CT state. As the currents of additives treated devices in the forward bias were generally larger as compared to the same devices without any additives, the recombination of devices with additives might occur more strongly through nonradiative pathways such as, e.g., triplet states. The origin of this deviation from the reciprocity relation is currently unclear and may rather be assigned to a change of injection properties than to changes of the morphology. However, via EL we were able to confirm the energy of the CT-state recombination that was observed already in the PL-spectra of the blends (Figure 7b).

The surface topology of the active layers was investigated by means of tapping mode atomic force microscopy (AFM) in order to further elucidate possible changes upon application of additives. Figure 8 summarizes the results obtained on films spin coated from the pure BTD-F-DKPP terpolymer (Figure 8a), BTD-F-DKPP:PCBM without additives (Figure 8b), and with the solvent additives hexane (8c), thiophene (8d), methanol (8e), and DMSO (8f). The pristine BTD-F-DKPP copolymer films (a) are continuous and relatively featureless. In contrast, terpolymer:fullerene films (b) exhibited some larger structures indicating phase separation with PCBM. The surface topography of the blend films processed with the additives thiophene (d) and methanol (e) did not show significant changes as compared to the pristine blend (b). Interestingly the blends modified with hexane (c) exhibited a somewhat smaller

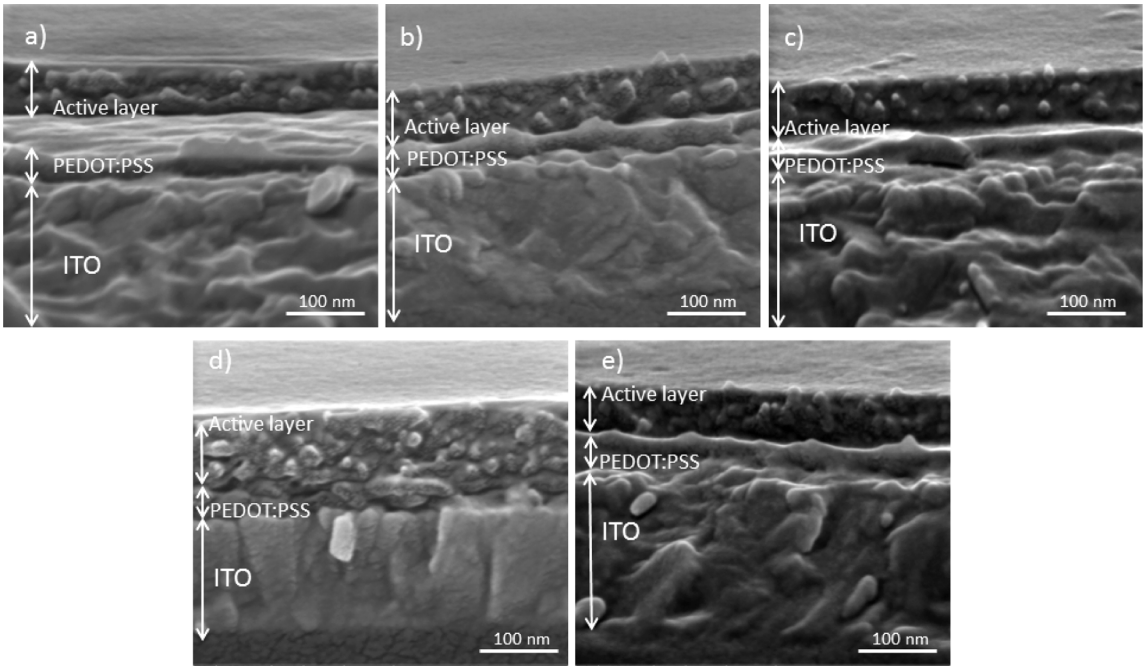

Figure 9. SEM cross-sectional view of BTD-F-DKPP:PCBM without (a) and with hexane (b), thiophene (c), methanol (d), and DMSO (e) additives spin-cast on top of ITO/PEDOT:PSS layers.

Table 2. Photovoltaic Performance of BHJ Solar Cells Composed of Identically Processed BTD-F-DKPP:PCBM Active Layers on Top of PEDOT:PSS Layers That Were Modified by Various Processing Additives (EQE Corrected Data)

PEDOT:PSS treatment by	dipole moment (C·m)	boiling point (°C)	J_{sc} (mA/cm^2)	V_{oc} (mV)	FF (%)	PCE (%)	PCE max (%)	R_s (Ω)	R_p (Ω)
none			3.3 ± 0.1	551 ± 5	41.8 ± 1.0	0.77 ± 0.01	0.78	9	925
hexane	0.0	68	4.3 ± 0.1	625 ± 7	41.2 ± 1.0	1.01 ± 0.01	1.02	6	718
thiophene	1.6	84	4.4 ± 0.1	636 ± 5	41.6 ± 3.0	1.17 ± 0.02	1.19	6.9	672
methanol	5.5	65	4.7 ± 0.1	689 ± 3	41.0 ± 1.0	1.23 ± 0.02	1.25	6.3	590
DMSO	13.0	189	4.8 ± 0.2	721 ± 10	39.1 ± 2.0	1.38 ± 0.01	1.39	6.8	550

phase separation. However, the AFM images of the blend films processed with DMSO (f) exhibited a considerable decrease in the phase separation, reminiscent to the topography of the pure terpolymer film, indicating a polymer wetting layer on top of the films. This wetting layer is in good agreement with the observation of a considerably lower fill factor of corresponding solar cells as well as the additional terpolymer PL feature found for these blends (compare with Figure 4b).

The possible bulk morphology modifications upon additives treatment were further investigated by SEM measurements. Figure 9 summarizes the results obtained on films spin coated from BTD-F-DKPP:PCBM without additives (Figure 9a) and with the solvent additives hexane (Figure 9b), thiophene (Figure 9c), methanol (Figure 9d), and DMSO (Figure 9e) on top of ITO/PEDOT:PSS layers. The SEM images revealed no difference in bulk morphology for films without (Figure 9a) any additives as well as for thiophene(Figure 9c) and methanol (Figure 9d) treatments, which is in agreement with AFM measurements. Upon treatment by hexane (Figure 9b), the scale of phase separation is somewhat smaller compared to the untreated film. Furthermore, the SEM images of the blend films processed with DMSO (e) exhibited small variations in film morphology, which can be correlated with revealed by AFM changes. Thereby, according to SEM and AFM measurements the morphological changes—if any—upon active layer modification by additives cannot cause significant changes in the device performance.

As neither the optical characterization nor the AFM and SEM measurements revealed significant changes between the films without and with additives—except for DMSO—the improved device performance might be attributed dominantly to another effect than morphological changes in general. One remaining possibility is a modification of the lower interface of the photoactive layer with PEDOT:PSS. In order to verify this hypothesis, we selectively treated the PEDOT:PSS layer using these four solvent additives. Therefore, hexane, thiophene, methanol and DMSO were spin-cast on top of the previously annealed PEDOT:PSS layer. The results for the corresponding solar cell performance including device-to-device variation collected from ∼150 devices per parameter are summarized in Table 2.

Introduction of the chosen additive solvents, by spin coating on top of the PEDOT:PSS layer, significantly improved the solar cell performance, but not to the extent that was observed in the case of using additives. A considerable increase was determined for both, the photocurrent and the open circuit voltage which resulted in increased solar cells efficiencies. The performance improvement was found to be linearly dependent on the additives dipole moments. While the obtained photocurrents were even higher than for the devices with additives, the open circuit voltage increase was lower and no

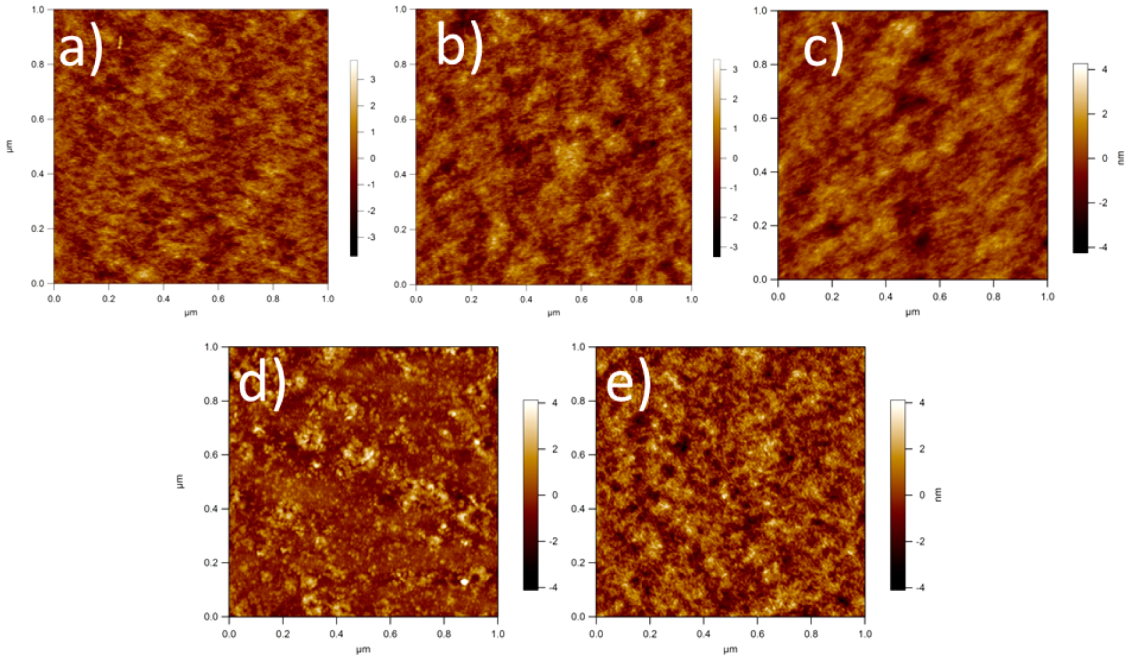

Figure 10. AFM images of the PEDOT:PSS films (a) not treated, and with top-cast (b) hexane, (c) thiophene, (d) methanol, and (e) DMSO.

improvement in fill factor was found. As only the interface between PEDOT:PSS and the blend film was modified, the improvement in photocurrent and photovoltage has to be assigned to a reduced charge extraction barrier for holes accompanied by a reduction in interfacial charge recombination, otherwise limiting the obtainable open circuit voltage.[51] The deviation of the device performance based on the PEDOT:PSS top-cast treatment alone as compared to the solvent addition to the active layer solution therefore has to be assigned to additional beneficial changes occurring at the active layer/metal interface, as reported by Wang et al.[41] and Zhou et al.[39]

As changes at the interface on top of the PEDOT:PSS layer should be visible by topography measurements, PEDOT:PSS films treated by solvents were characterized by tapping mode AFM (Figure 10). No differences are visible comparing the untreated film (Figure 10a) and the hexane (Figure 10b) and thiophene treated films (Figure 10c). However, for the methanol (Figure 10d) and DMSO (Figure 10e) treated PEDOT:PSS films significant changes became obvious. Methanol treated PEDOT:PSS exhibited small exposed grainy structures while treatment with DMSO resulted in fibrillar ones. In order to gain additional information about these morphological changes at the PEDOT:PSS surface, we applied X-ray and ultraviolet photoelectron spectroscopy (XPS, UPS) to characterize changes in surface composition and electronic properties.

Indeed the XPS and UPS measurements confirmed changes of the PEDOT:PSS surface after treatment by additives. Figures 11 and 12 show the XPS and UPS spectra for treated PEDOT:PSS films. A clear variation of the surface stoichiometry was observed. The chemical states in the O 1s, C 1s and S 2p spectra, shown in Figure 11, can be assigned to different chemical bonds within the PEDOT and PSS molecular structures[54,55] as labeled for each core level. PEDOT:PSS treatment with hexane or thiophene resulted only in minor changes between the ratio of PSS sulfonic and PEDOT sulfur groups as compared to untreated PEDOT:PSS. A reduction of

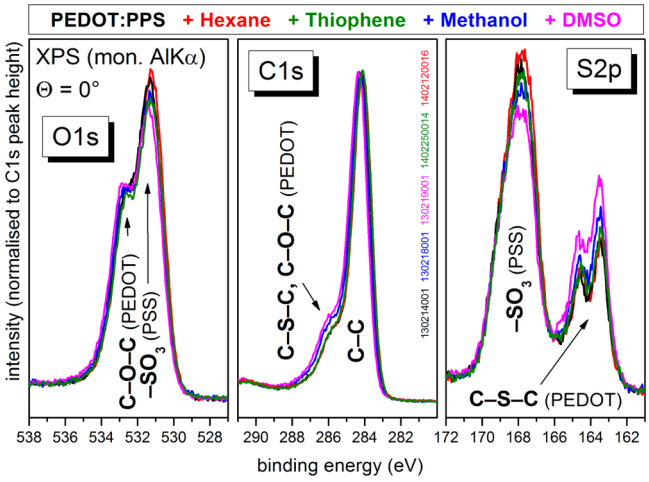

Figure 11. XPS measurements of the O 1s, C 1s, and S 2p core levels for untreated PEDOT:PSS films and identical PEDOT:PSS films with additional spin-coating of methanol, DMSO, thiophene, or hexane (relative intensities normalized with respect to the C 1s peak height). The C 1s spectra of untreated, thiophene, or hexane treated PEDOT:PSS are practically identical.

the sulfonic group from PSS after thiophene (−4%), methanol (−11%), or DMSO (−18%) treatment is visible in the S 2p spectra, while in parallel an enhancement of the amount PEDOT sulfur groups was found (+8% for thiophene, +19% for methanol, and +40% for DMSO). For the hexane treatment, only minor changes in the surface composition are observed. Corresponding trends are also visible for related functional groups in the C 1s and O 1s signals unveiling that especially for treatments with methanol and DMSO, the concentration of PEDOT is enhanced near the surface while the signal related to PSS is decreased. The insulating PSS seems to be washed out near the surface of the PEDOT:PSS layer, resulting in an enrichment of the positively charged and highly conductive PEDOT phase. Similar effects have already been observed for

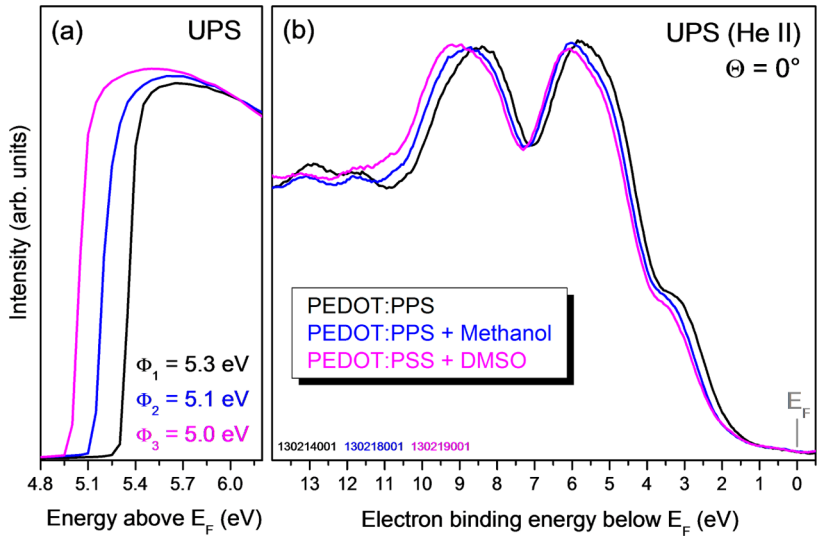

Figure 12. Ultraviolet photoelectron spectra of PEDOT:PSS without and with additional treatment with methanol or DMSO. (a) Measurement of the onset of electron emission, equivalent to the vacuum level position, for determination of the work function $\Phi = E_{Vac} - E_F$. An external sample bias of −2 V was applied to measure the true secondary electron onset. (b) He II spectra of the valence electron region (occupied states below E_F).

other solvent treatments.[56] The film thickness measurement of PEDOT:PSS layers before and after modification by solvent additives indeed confirmed a reduction from initially 30 nm (untreated) to 28 nm (hexane, thiophene), to 25 nm (methanol), or even down to 22 nm (DMSO).

Since such compositional changes as for methanol and DMSO are expected to modify the electronic properties of the PEDOT:PSS film surface and such the interface with other materials, UPS measurements for methanol and DMSO treated PEDOT:PSS films were performed. The analysis of the low kinetic energy onset of electron emission (Figure 12a) revealed that the work function of the PEDOT:PSS layer was increased upon the annealing step at 180 °C from 5.0 to 5.3 eV (not shown). In case the samples were additionally treated by a solvent, the work function was lowered to 5.1 eV for methanol and 5.0 eV for DMSO, thus thwarting the annealing effect. The enrichment of the positively charged PEDOT phase at the surface resulted in a modification of the surface charge distribution, thus lowering the work function.[55]

The measured valence band structure as shown in Figure 12b is in excellent agreement with earlier studies of PEDOT:PSS films.[56] Interestingly, the occupied states, as referred to the Fermi level E_F in such photoemission experiments, slightly shift to higher binding energy (BE) by 0.2−0.3 eV after solvent treatment. A comparable change of core level BE is also observed in the corresponding XPS spectra shown in Figure 11, best visible in the C 1s spectra.

The parallel variation of both, work function and electronic binding energy, upon solvent treatment indicates a shift of the Fermi level toward the vacuum level E_{Vac} of the material. At the same time the energy position of the occupied states and consequently also the unoccupied states remained unaffected when referred to E_{Vac}. It is anticipated that the partial removal of the PSS-phase has consequences on the density of occupied and unoccupied electronic states within the PEDOT-phase, resulting in a slight modification of the Fermi level position within the band of occupied states. Similar trends have also been calculated by density function theory.[57] Since no change in the energy level of occupied states (referred to E_{Vac}) was observed in the UPS and XPS measurements, no dipole formation between the bulk PEDOT:PSS and PSS-enriched surface layer upon treatment by methanol or DMSO takes place. The open circuit voltage of the solar cells is strongly dependent on the relative position of the active layer bulk heterojunction Fermi level with respect to the Fermi level of the PEDOT:PSS. The larger the difference between both, the larger will be the expected band bending or correspondingly the interfacial dipole upon Fermi level alignment. The band diagram in Figure 13 may explain the simultaneously increased

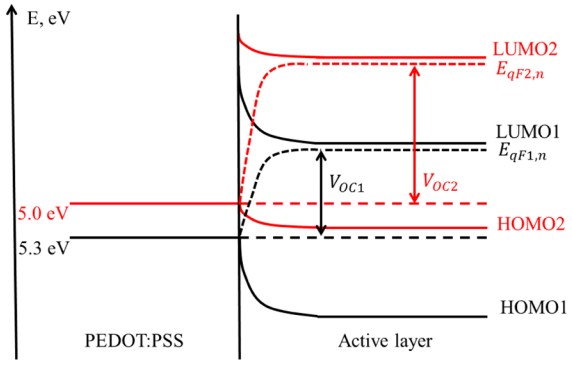

Figure 13. Schematic energy band diagram of the interface between PEDOT:PSS and the active layer, before (black lines) and after solvent treatment (red lines) of the PEDOT:PSS film. A smaller shift between the HOMO of the active layer and the PEDOT:PSS work function—as obtained upon solvent treatment—will result in reduced energy losses and consequently lead to an increase of the open circuit voltage.

short circuit current and open circuit voltage upon PEDOT:PSS treatment. For organic semiconductors E_F is generally located within the band gap—respectively between HOMO and LUMO level—between 4 and 5 eV.[58] In the case of treated PEDOT:PSS (red lines) the lowered work function may result in a smaller band bending as compared with untreated (annealed) PEDOT:PSS (black lines), exhibiting a higher work function. As a result, upon solvent treatment, the band bending (or dipolar shifts) within the photoactive layer associated with the Fermi level equilibration are decreased, leading straightforward to an increase of the open circuit

Table 3. Photovoltaic Performance of BHJ Solar Cells Composed of PCDTBT:PCBM Fabricated with Various Processing Additives (EQE Corrected Data) Including Device-to-Device Variation

PCDTBT: PCBM + additive	dipole moment (C·m)	boiling point (°C)	J_{sc} (mA/cm^2)	V_{oc} (mV)	FF (%)	PCE (%)	PCE max (%)	R_s (Ω)	R_p (Ω)
chlorobenzene (host solvent)	5.2	131	10.1 ± 0.1	832 ± 4	51.2 ± 1.0	4.52 ± 0.04	4.56	5.7	1024
hexane	0.0	68	10.2 ± 0.3	835 ± 5	51.6 ± 2.0	4.67 ± 0.05	4.72	6.5	974
thiophene	1.6	84	10.5 ± 0.2	859 ± 3	50.0 ± 1.0	4.65 ± 0.04	4.69	7.9	901
methanol	5.5	65	10.2 ± 0.2	914 ± 4	55.2 ± 2.0	5.33 ± 0.04	5.37	6.0	1107
DMSO	13.0	189	10.3 ± 0.5	901 ± 2	52.8 ± 3.0	5.20 ± 0.06	5.26	4.7	1136

voltage. Notably, in case of accounting only the holes extracting electrode work function, this would be rather unexpected. However, the experimental results showed that energy level adaptation at the active layer/PEDOT:PSS interface plays a major role here.

Various studies have confirmed that different solvent treatments of PEDOT:PSS result in a rearrangement of the conductive PEDOT network within the insulating PSS host. This includes reorientation of the PEDOT:PSS chains,[59] enhancing the conduction of charge carriers due to the formation of 3D PEDOT:PSS networks,[60] aggregation of PEDOT,[61,62] inducing screening effects between PEDOT and PSS by high boiling point solvents,[63] removal of PSS between the conductive PEDOT grains,[57,64] and rearrangement from aggregated to linear or expanded-aggregated polymer chains with the addition of DMSO or ethylene glycol.[65,66] Our study confirms the partial removal of PSS from the surface inducing a change in the morphology of the PEDOT accompanied by modified electronic properties.

We conclude that this reduction of the insulating PSS surface causes a decrease of the energy barrier for hole extraction from the active layer, which in consequence could be related to the photocurrent increase. Additionally, the energy level alignment at the interface between PEDOT:PSS and the active layer resulted in smaller energy losses upon PEDOT:PSS modification, which consequently increased the open circuit voltage and thus might be one reason for the improvement of the solar cell performance. This effect seems to be fully valid for spinning the additive directly onto the PEDOT:PSS layer and partially for incorporating the polar additive into the active layer solution.

To confirm the beneficial effect of solvent additive treatments and to prove its applicability to other material systems, we investigated another low-bandgap polymer poly[*N*-900-hepta-decanyl-2,7-carbazole-*alt*-5,5-(40,70-di-2-thienyl-20,10,30-benzothiadiazole)] (PCDTBT) in similarly processed solar cells. Incorporation of the additives into the active layer solution indeed demonstrated increase of the solar cells efficiency based on PCDTBT:$PC_{70}BM$. The experimental data, respectively photovoltaic parameters are shown in Table 3. Indeed, especially methanol, which positive influence on high performing solar cells was recently shown,[39] and DMSO resulted in the largest improvements of the overall performance by 15−18%, which was reflected in each photovoltaic parameters increase, of otherwise identically processed active layers. BTD-F-DKPP-based devices generally revealed a higher level of performance improvement comparing with PCDTBT-based solar cells. This might be attributed to an additional positive effect of additives on BTD-F-DKPP terpolymer as washing out impurities, which could remain after polymerization process.

In this study, an increase of the device performance can be partly assigned to a change of the PEDOT:PSS-active layer interface. However, we have observed a lower increase of the open circuit voltage and no increase in the fill factor in case of devices with selectively treated by polar solvents PEDOT:PSS electrode as compared to additives approach. Therefore, we assume that another part of the observed improvement in the solar cell performance for active layers processed with polar solvent additives can be assigned to a modification of the organic/metal interface which was observed earlier by Liu et al.,[40] Zhou et al.,[39] and Wang et al.,[41] resulting in a passivation of surface traps and in a decrease of the surface recombination rate. In conclusion, our study complements and extends beyond the formerly reported investigations on the effect of polar solvent treatments and ultimately enables to draw a more complete picture.

4. SUMMARY AND CONCLUSION

We demonstrated the successful application of different polar solvent additives to BTD-F-DKPP:PCBM bulk heterojunction solar cells resulting in an improvement of the overall solar cell performance. Whereas earlier works demonstrated performance improvements of various material systems upon methanol top-cast treatments, we have specifically introduced a more processing-friendly variant by adding the methanol into the active layer solution, resulting in similar or even larger performance improvements. Furthermore, by variation of the additive solvents dipole moment, we observed a correlation between the magnitude of the dipole moment of additives and their optimum concentration within the photoactive layer solution: generally a larger dipole moment of the additive required less concentration to yield optimum performance. Detailed investigation of optical properties and surface topography and morphology of the polymer:fullerene films did not show any change upon additives treatment—except for DMSO and (less pronounced) hexane.

Surface analysis by UPS and XPS measurements demonstrated that the direct top-cast treatment of annealed PEDOT:PSS layers by the same additive solvents results in changes of the surface chemical composition and consequently its electronic properties by a partial removal of insulating PSS. Topography measurements confirmed these conformational changes especially for methanol and DMSO. Partial removal of the PSS resulted in a change of the PEDOT:PSS work function and its energy level alignment with the active layer. This reduced potential energy losses by decreasing the energy barrier for charge carrier extraction, resulting in improved photocurrents and open circuit voltages. However, by treatment of the PEDOT:PSS layer alone, only part of the device improvement connected to additives could be realized. Hence the difference between PEDOT:PSS solvent treatment and additives in the active layer formulation may be assigned to

reduced recombination at the electron extracting electrode, as reported earlier. Thus, we do provide additional to existing earlier information about the positive effects arising from the application of methanol, which is not only the surface effects on the photoactive layer but also the specific changes of the PEDOT:PSS interface. In addition, we could reproduce the beneficial effect of these polar solvent additives for PCDTBT-based polymer solar cells, confirming the effect to be rather independent of the material system applied.

AUTHOR INFORMATION

Corresponding Authors

*E-mail: olesia.synooka@tu-ilmenau.de (O.S.).
*E-mail: harald.hoppe@tu-ilmenau.de (H.H.).

Notes

The authors declare no competing financial interest.

ACKNOWLEDGMENTS

O.S. gratefully acknowledges financial support by the Federal state of Thuringia via Landesgraduierten Förderung Thüringen and Thüringische Landesgraduiertenschule für Photovoltaik (PhotoGrad). Additionally, we gratefully acknowledge fruitful discussion with R. Rösch, R. Öttking, and, especially, W. J. D. Beenken (Technische Universität Ilmenau). F.L. thanks the Max Planck Society for funding the Max Planck Research Group of Organic Optoelectronics and the Deutsche Forschungsgemeinschaft (DFG) for funding in the framework of the priority program SPP1355 "Elementary Processes in Organic Photovoltaics". D.G. acknowledges a Kekulé scholarship of the Fonds der Chemischen Industrie (FCI). M.H. and S.K. are grateful for research cofunding by the state of Thuringia and the European Union (ESF) under grant number 2012 FGR 0231.

REFERENCES

(1) Krebs, F. C.; Jørgensen, M.; Norrman, K.; Hagemann, O.; Alstrup, J.; Nielsen, T. D.; Fyenbo, J.; Larsen, K.; Kristensen, J. A Complete Process for Production of Flexible Large Area Polymer Solar Cells Entirely Using Screen Printing—First Public Demonstration. *Sol. Energy Mater. Sol. Cells.* **2009**, *93*, 422−441.

(2) Nielsen, T. D.; Cruickshank, C.; Foged, S.; Thorsen, J.; Krebs, F. C. Business, Market and Intellectual Property Analysis of Polymer Solar Cells. *Sol. Energy Mater. Sol. Cells.* **2010**, *94*, 1553−1571.

(3) Li, G.; Zhu, R.; Yang, Y. Polymer Solar Cells. *Nat. Photonics* **2012**, *6*, 153−161.

(4) Kumar, P.; Chand, S. Recent Progress and Future Aspects of Organic Solar Cells. *Prog. Photovoltaics: Res. Appl.* **2012**, *20*, 377−415.

(5) Darling, S. B.; You, F. The Case for Organic Photovoltaics. *RSC Adv.* **2013**, *3*, 17633−17648.

(6) Green, M. A.; Emery, K.; Hishikawa, Y.; Warta, W.; Dunlop, E. D. Solar Cell Efficiency Tables (version 43). *Prog. Photovoltaics: Res. Appl.* **2014**, *22*, 1−9.

(7) Zervos, H.; Das, R.; Ghaffarzadeh, K. *Organic Photovoltaics (OPV) 2013−2023: Technologies, Markets, Players*; IDTechEx, 2014.

(8) Sariciftci, N. S.; Smilowitz, L.; Heeger, A. J.; Wudl, F. Photoinduced Electron Transfer from a Conducting Polymer to Buckminsterfullerene. *Science* **1992**, *258*, 1474−1476.

(9) Yu, G.; Gao, J.; Hummelen, J. C.; Wudl, F.; Heeger, A. J. Polymer Photovoltaic Cells: Enhanced Efficiencies via a Network of Internal Donor-Acceptor Heterojunctions. *Science* **1995**, *270*, 1789−1791.

(10) Hoppe, H.; Sariciftci, N. S. Morphology of Polymer/Fullerene Bulk Heterojunction Solar Cells. *J. Mater. Chem.* **2006**, *16*, 45−61.

(11) Ltaief, A.; Davenas, J.; Bouazizi, A.; Ben Chaâbane, R.; Alcouffe, P.; Ben Ouada, H. Film Morphology Effects on the Electrical and Optical Properties of Bulk Heterojunction Organic Solar Cells Based on MEH-PPV/C60 Composite. *Mater. Sci. Eng. C* **2005**, *25*, 67−75.

(12) Chen, W.; Nikiforov, M. P.; Darling, S. B. Morphology Characterization in Organic and Hybrid Solar Cells. *Energy Environ. Sci.* **2012**, *5*, 8045−8074.

(13) Liu, F.; Gu, Y.; Shen, X.; Ferdous, S.; Wang, H.-W.; Russell, T. P. Characterization of the Morphology of Solution-Processed Bulk Heterojunction Organic Photovoltaics. *Prog. Polym. Sci.*. **2013**, *38*, 1990−2052.

(14) Wang, D. H.; Moon, J. S.; Seifter, J.; Jo, J.; Park, J. H.; Park, O. O.; Heeger, A. J. Sequential Processing: Control of Nanomorphology in Bulk Heterojunction Solar Cells. *Nano Lett.* **2011**, *11*, 3163−3168.

(15) Hoppe, H.; Niggemann, M.; Winder, C.; Kraut, J.; Hiesgen, R.; Hinsch, A.; Meissner, D.; Sariciftci, N. S. Nanoscale Morphology of Conjugated Polymer/Fullerene-Based Bulk- Heterojunction Solar Cells. *Adv. Funct. Mater.* **2004**, *14*, 1005−1011.

(16) Zhao, Y.; Xie, Z.; Qu, Y.; Geng, Y.; Wang, L. Solvent-Vapor Treatment Induced Performance Enhancement of Poly(3-hexylthiophene):Methanofullerene Bulk-Heterojunction Photovoltaic Cells. *Appl. Phys. Lett.* **2007**, *90*, 43504−1−3.

(17) Zhao, Y.; Guo, X.; Xie, Z.; Qu, Y.; Geng, Y.; Wang, L. Solvent Vapor-Induced Self Assembly and its Influence on Optoelectronic Conversion of Poly(3-hexylthiophene): Methanofullerene Bulk Heterojunction Photovoltaic Cells. *J. Appl. Polym. Sci.* **2009**, *111*, 1799−1804.

(18) Ko, C.-J.; Lin, Y.-K.; Chen, F.-C. Microwave Annealing of Polymer Photovoltaic Devices. *Adv. Mater.* **2007**, *19*, 3520−3523.

(19) Padinger, F.; Rittberger, R. S.; Sariciftci, N. S. Effects of Postproduction Treatment on Plastic Solar Cells. *Adv. Funct. Mater.* **2003**, *13*, 85−88.

(20) Synooka, O.; Eberhardt, K.-R.; Singh, C. R.; Hermann, F.; Ecke, G.; Ecker, B.; Hauff, E. von; Gobsch, G.; Hoppe, H. Influence of Thermal Annealing on PCDTBT:PCBM Composition Profiles. *Adv. Energy Mater.* **2013**, *4*, 1300981−1−14.

(21) Ma, W.; Yang, C.; Gong, X.; Lee, K.; Heeger, A. J. Thermally Stable, Efficient Polymer Solar Cells with Nanoscale Control of the Interpenetrating Network Morphology. *Adv. Funct. Mater.* **2005**, *15*, 1617−1622.

(22) Moulé, A. J.; Meerholz, K. Controlling Morphology in Polymer−Fullerene Mixtures. *Adv. Mater.* **2008**, *20*, 240−245.

(23) Brabec, C. J.; Heeney, M.; McCulloch, I.; Nelson, J. Influence of Blend Microstructure on Bulk Heterojunction Organic Photovoltaic Performance. *Chem. Soc. Rev.* **2011**, *40*, 1185−1199.

(24) Kästner, C.; Rathgeber, S.; Egbe, D. A. M.; Hoppe, H. Improvement of Photovoltaic Performance by Ternary Blending of Amorphous and Semi-Crystalline Polymer Analogues with PCBM. *J. Mater. Chem. A* **2013**, *1*, 3961−3969.

(25) Yao, Y.; Hou, J.; Xu, Z.; Li, G.; Yang, Y. Effects of Solvent Mixtures on the Nanoscale Phase Separation in Polymer Solar Cells. *Adv. Funct. Mater.* **2008**, *18*, 1783−1789.

(26) Ye, L.; Jing, Y.; Guo, X.; Sun, H.; Zhang, S.; Zhang, M.; Huo, L.; Hou, J. Remove the Residual Additives toward Enhanced Efficiency with Higher Reproducibility in Polymer Solar Cells. *J. Phys. Chem. C* **2013**, *117*, 14920−14928.

(27) Liao, H.-C.; Ho, C.-C.; Chang, C.-Y.; Jao, M.-H.; Darling, S. B.; Su, W.-F. Additives for Morphology Control in High-Efficiency Organic Solar Cells. *Mater. Today.* **2013**, *16*, 326−336.

(28) Dang, M. T.; Wuest, J. D. Using Volatile Additives to Alter the Morphology and Performance of Active Layers in Thin-Film Molecular Photovoltaic Devices Incorporating Bulk Heterojunctions. *Chem. Soc. Rev.* **2013**, *42*, 9105−23−26.

(29) Kim, M.; Kim, J.-H.; Choi, H. H.; Park, J. H.; Jo, S. B.; Sim, M.; Kim, J. S.; Jinnai, H.; Park, Y. D.; Cho, K. Solar Cells: Electrical Performance of Organic Solar Cells with Additive-Assisted Vertical Phase Separation in the Photoactive Layer. *Adv. Energy Mater.* **2014**, DOI: 10.1002/adma.201470010.

(30) Schmidt, K.; Tassone, C. J.; Niskala, J. R.; Yiu, A. T.; Lee, O. P.; Weiss, T. M.; Wang, C.; Fréchet, J. M. J.; Beaujuge, P. M.; Toney, M. F. A Mechanistic Understanding of Processing Additive-Induced

Efficiency Enhancement in Bulk Heterojunction Organic Solar Cells. *Adv. Mater.* **2014**, *26*, 300−305.
(31) Peet, J.; Kim, J. Y.; Coates, N. E.; Ma, W. L.; Moses, D.; Heeger, A. J.; Bazan, G. C. Efficiency Enhancement in Low-Bandgap Polymer Solar Cells by Processing with Alkane Dithiols. *Nat. Mater.* **2007**, *6*, 497−500.
(32) Peet, J.; Brocker, E.; Xu, Y.; Bazan, G. C. Controlled*β*-Phase Formation in Poly(9,9-di-n-octylfluorene) by Processing with Alkyl Additives. *Adv. Mater.* **2008**, *20*, 1882−1885.
(33) Lee, J. K.; Ma, W. L.; Brabec, C. J.; Yuen, J.; Moon, J. S.; Kim, J. Y.; Lee, K.; Bazan, G. C.; Heeger, A. J. Processing Additives for Improved Efficiency from Bulk Heterojunction Solar Cells. *J. Am. Chem. Soc.* **2008**, *130*, 3619−3623.
(34) Scharber, M. C.; Lungenschmied, C.; Egelhaaf, H.-J.; Matt, G.; Bednorz, M.; Fromherz, T.; Gao, J.; Jarzab, D.; Loi, M. A. Charge Transfer Excitons in Low Band Gap Polymer Based Solar Cells and the Role of Processing Additives. *Energy Environ. Sci.* **2011**, *4*, 5077−5083.
(35) Zhao, X.; Tang, H.; Yang, D.; Li, H.; Xu, W.; Yin, L.; Yang, X. Effect of Molecular Weight and Processing Additive on the Performance of Low Bandgap Polymer Solar Cells. *Chin. J. Chem.* **2012**, *30*, 2052−2058.
(36) Etzold, F.; Howard, I. A.; Forler, N.; Cho, D. M.; Meister, M.; Mangold, H.; Shu, J.; Hansen, M. R.; Müllen, K.; Laquai, F. The Effect of Solvent Additives on Morphology and Excited-State Dynamics in PCPDTBT:PCBM Photovoltaic Blends. *J. Am. Chem. Soc.* **2012**, *134*, 10569−10583.
(37) Salim, T.; Wong, L. H.; Bräuer, B.; Kukreja, R.; Foo, Y. L.; Bao, Z.; Lam, Y. M. Solvent Additives and Their Effects on Blend Morphologies of Bulk Heterojunctions. *J. Mater. Chem.* **2010**, *21*, 242−250.
(38) Seo, J. H.; Gutacker, A.; Sun, Y.; Wu, H.; Huang, F.; Cao, Y.; Scherf, U.; Heeger, A. J.; Bazan, G. C. Improved High-Efficiency Organic Solar Cells via Incorporation of a Conjugated Polyelectrolyte Interlayer. *J. Am. Chem. Soc.* **2011**, *133*, 8416−8419.
(39) Zhou, H.; Zhang, Y.; Seifter, J.; Collins, S. D.; Luo, C.; Bazan, G. C.; Nguyen, T.-Q.; Heeger, A. J. High-Efficiency Polymer Solar Cells Enhanced by Solvent Treatment. *Adv. Mater.* **2013**, *25*, 1646−1652.
(40) Liu, X.; Wen, W.; Bazan, G. C. Post-Deposition Treatment of an Arylated-Carbazole Conjugated Polymer for Solar Cell Fabrication. *Adv. Mater.* **2012**, *24*, 4505−4510.
(41) Wang, Q.; Zhou, Y.; Zheng, H.; Shi, J.; Li, C.; Su, C. Q.; Wang, L.; Luo, C.; Hu, D.; Pei, J.; Wang, J.; Peng, J.; Cao, Y. Modifying Organic/Metal Interface via Solvent Treatment to Improve Electron Injection in Organic Light Emitting Diodes. *Org. Electron.* **2011**, *12*, 1858−1863.
(42) Sonar, P.; Ng, G.-M.; Lin, T. T.; Dodabalapur, A.; Chen, Z.-K. Solution Processable Low Bandgap Diketopyrrolopyrrole (DPP) Based Derivatives: Novel Acceptors for Organic Solar Cells. *J. Mater. Chem.* **2010**, *20*, 3626−3636.
(43) Liu, F.; Gu, Y.; Wang, C.; Zhao, W.; Chen, D.; Briseno, A. L.; Russell, T. P. Efficient Polymer Solar Cells Based on a Low Bandgap Semi-crystalline DPP Polymer-PCBM Blends. *Adv. Mater.* **2012**, *24*, 3947−3951.
(44) Kretschmer, F.; Hager, M. D.; Synooka, O.; Hoppe, H.; Schubert, U. S. *Donor-acceptor π-conjugated polymer libraries for polymer solar cells* **2012**, submitted for publication.
(45) Liptay, W. Tables of Experimental Dipole Moments. *Angew. Chem.* **1965**, *77*, 276.
(46) Murgatroyd, P. N. Theory of Space-Charge-Limited Current Ehanced by Frenkel Effect. *J. Phys. D: Appl. Phys.* **1970**, *3*, 151−156.
(47) Himmerlich, M.; Krischok, S.; Lebedev, V.; Ambacher, O.; Schaefer, J. A. Morphology and Surface Electronic Structure of MBE Grown InN. *J. Cryst. Growth.* **2007**, *306*, 6−11.
(48) Opitz, A.; Bronner, M.; Brütting, W.; Himmerlich, M.; Schaefer, J. A.; Krischok, S. Electronic Properties of Organic Semiconductor Blends: Ambipolar Mixtures of Phthalocyanine and Fullerene. *Appl. Phys. Lett.* **2007**, *90*, 212112−1−3.
(49) Hallermann, M.; Kriegel, I.; Da Como, E.; Berger, J. M.; Hauff, E. von; Feldmann, J. Charge Transfer Excitons in Polymer/Fullerene Blends: The Role of Morphology and Polymer Chain Conformation. *Adv. Funct. Mater.* **2009**, *19*, 3662−3668.
(50) Kästner, C.; Muhsin, B.; Wild, A.; Egbe, D. A. M.; Rathgeber, S.; Hoppe, H. Improved Phase Separation in Polymer Solar Cells by Solvent Blending. *J. Polym. Sci., Part B: Polym. Phys.* **2013**, *51*, 868−874.
(51) Singh, C. R.; Sommer, M.; Himmerlich, M.; Wicklein, A.; Krischok, S.; Thelakkat, M.; Hoppe, H. Morphology Controlled Open Circuit Voltage in Polymer Solar Cells. *Phys. Status Solidi RRL.* **2011**, *5*, 247−249.
(52) Rau, U.; Werner, J. H. Radiative Efficiency Limits of Solar Cells with Lateral Band-gap Fluctuations. *Appl. Phys. Lett.* **2004**, *84*, 3735−3737.
(53) Veldman, D.; İpek, Ö.; Meskers, S. C. J.; Sweelssen, J.; Koetse, M. M.; Veenstra, S. C.; Kroon, J. M.; van Bavel, S. S.; Loos, J.; Janssen, R. A. J. Compositional and Electric Field Dependence of the Dissociation of Charge Transfer Excitons in Alternating Polyfluorene Copolymer/Fullerene Blends. *J. Am. Chem. Soc.* **2008**, *130*, 7721−7735.
(54) Greczynski, G.; Kugler, T.; Keil, M.; Osikowicz, W.; Fahlman, M.; Salaneck, W. Photoelectron Spectroscopy of Thin Films of PEDOT−PSS Conjugated Polymer Blend: a Mini-review and some New Results. *J. Electron Spectrosc. Relat. Phenom.* **2001**, *121*, 1−17.
(55) Koch, N.; Vollmer, A.; Elschner, A. Influence of Water on the Work Function of Conducting Poly(3,4-ethylenedioxythiophene)/Poly(styrenesulfonate). *Appl. Phys. Lett.* **2007**, *90*, 43512-1−43512-3.
(56) Jönsson, S.; Birgerson, J.; Crispin, X.; Greczynski, G.; Osikowicz, W.; Denier van der Gon, A. W.; Salaneck, W.; Fahlman, M. The Effects of Solvents on the Morphology and Sheet Resistance in Poly(3,4-ethylenedioxythiophene)−Polystyrenesulfonic Acid (PEDOT−PSS) Films. *Synt. Met.* **2003**, *139*, 1−10.
(57) Lenz, A.; Kariis, H.; Pohl, A.; Persson, P.; Ojamäe, L. The Electronic Structure and Reflectivity of PEDOT:PSS from Density Functional Theory. *Chem. Phys.* **2011**, *384*, 44−51.
(58) Hoppe, H.; Glatzel, T.; Niggemann, M.; Hinsch, A.; Lux-Steiner, M. C.; Sariciftci, N. S. Kelvin Probe Force Microscopy Study on Conjugated Polymer/Fullerene Bulk Heterojunction Organic Solar Cells. *Nano Lett.* **2005**, *5*, 269−274.
(59) Pettersson, L. A.; Ghosh, S.; Inganäs, O. Optical Anisotropy in Thin Films of Poly(3,4-ethylenedioxythiophene)−Poly(4-styrenesulfonate). *Org. Electron.* **2002**, *3*, 143−148.
(60) Ashizawa, S.; Horikawa, R.; Okuzaki, H. Effects of Solvent on Carrier Transport in Poly(3,4-ethylenedioxythiophene)/Poly(4-styrenesulfonate). *Synt. Met.* **2005**, *153*, 5−8.
(61) Timpanaro, S.; Kemerink, M.; Touwslager, F. J.; de Kok, M. M.; Schrader, S. Morphology and Conductivity of PEDOT/PSS Films Studied by Scanning−Tunneling Microscopy. *Chem. Phys. Lett.* **2004**, *394*, 339−343.
(62) Snaith, H. J.; Kenrick, H.; Chiesa, M.; Friend, R. H. Morphological and Electronic Consequences of Modifications to the Polymer Anode 'PEDOT:PSS'. *Polymer.* **2005**, *46*, 2573−2578.
(63) Kim, J. Y.; Jung, J. H.; Lee, D. E.; Joo, J. Enhancement of Electrical Conductivity of Poly(3,4-ethylenedioxythiophene)/Poly(4-styrenesulfonate) by a Change of Solvents. *Synt. Met.* **2002**, *126*, 311−316.
(64) Crispin, X.; Marciniak, S.; Osikowicz, W.; Zotti, G.; van der Gon, A. W. D.; Louwet, F.; Fahlman, M.; Groenendaal, L.; de Schryver, F.; Salaneck, W. R. Conductivity, Morphology, Interfacial Chemistry, and Stability of Poly(3,4-ethylene dioxythiophene)-Poly-(styrene Sulfonate): A Photoelectron Spectroscopy Study. *J. Polym. Sci. B Polym. Phys.* **2003**, *41*, 2561−2583.
(65) Ouyang, J.; Xu, Q.; Chu, C.-W.; Yang, Y.; Li, G.; Shinar, J. On the Mechanism of Conductivity Enhancement in Poly(3,4-ethylenedioxythiophene):Poly(styrene sulfonate) Film Through Solvent Treatment. *Polymer.* **2004**, *45*, 8443−8450.

(66) Bagchi, D.; Menon, R. Conformational Modification of Conducting Polymer Chains by Solvents: Small-angle X-ray Scattering Study. *Chem. Phys. Lett.* **2006**, *425*, 114−117.